


Communication

# An Alternative Method to Determine the Quantum Yield of the Excited Triplet State Using Laser Flash Photolysis

Iouri Evgenievitch Borissevitch <sup>1,2,\*</sup> , Eli Silveira-Alves, Jr. <sup>3</sup> , Claudio Gabriel Lemos Almeida <sup>4</sup> ,  
Guilherme Rocha Lino Souza <sup>5</sup>, Svyatoslav Sergeevich Sokolov <sup>6</sup> and Pablo José Gonçalves <sup>2,3,\*</sup> 

<sup>1</sup> Departamento de Física, Faculdade de Filosofia, Ciências e Letras de Ribeirão Preto, Universidade de São Paulo, Ribeirão Preto 14040-901, Brazil

<sup>2</sup> Instituto de Física, Universidade Federal de Goiás, Goiânia 74690-900, Brazil

<sup>3</sup> Instituto de Química, Universidade Federal de Goiás, Goiânia 74690-900, Brazil

<sup>4</sup> Escola de Engenharia Elétrica, Mecânica e de Computação, Universidade Federal de Goiás, Goiânia 74690-900, Brazil

<sup>5</sup> Instituto de Ciências Biológicas, Universidade Federal de Goiás—UFG, Goiânia 74690-900, Brazil

<sup>6</sup> B. Verkin Institute for Low Temperature Physics and Engineering of the National Academy of Sciences of Ukraine 47 Nauky Ave, 61103 Kharkiv, Ukraine

\* Correspondence: iourib@ffclrp.usp.br (I.E.B.); pablo@ufg.br (P.J.G.)

**Abstract:** The excited triplet state of a molecule ( $T_1$ ) is one of the principal intermediate products in various photochemical processes due to its high reactivity and relatively long lifetime. The  $T_1$  quantum yield ( $\phi_T$ ) is one of the most important characteristics in the study of photochemical reactions. It is of special interest to determine the  $\phi_T$  of various photoactive compounds (photosensitizer, PS) used in photodynamic therapy (PDT). PDT is an effective medical technique for the treatment of serious diseases, such as cancer and bacterial, fungal and viral infections. This technique is based on the introduction of a PS to a patient's organism and its further excitation by visible light, producing reactive oxygen species (ROS) via electron or energy transfer from the PS  $T_1$  state to the biological substrate or molecular oxygen. Therefore, information on the  $\phi_T$  value is fundamental in the search for new and effective PSs. There are various experimental methods to determine  $\phi_T$  values; however, these methods demonstrate a high discrepancy between  $\phi_T$  values. This stimulates the analysis of various factors that can affect the determined  $\phi_T$ . In this study, we analyze the effect of the intensity profile of the exciting laser pulse on the calculation of the  $\phi_T$  value obtained by the Laser Flash Photolysis technique. The  $\phi_T$  values were determined by analyzing the variation of a sample transient absorption in the function of the exciting laser pulse intensity, in combination with the spectral and kinetic PS characteristics obtained in nonlinear optical experiments by solving the rate equations of a five-level-energy diagram. Well-studied PSs: *meso*-tetra(4-sulfonatophenyl) (TPPS<sub>4</sub>) porphyrins, its zinc complex (ZnTPPS<sub>4</sub>) and the zinc complex of *meso*-tetrakis(N-methylpyridinium-4-yl) (ZnTMPyP) were chosen as test compounds to evaluate the proposed model. The  $\phi_T$  values were determined through a comparison with the  $\phi_{T,TMPyP} = 0.82$  of *meso*-tetrakis(N-methylpyridinium-4-yl) (TMPyP), used as a standard. The obtained results ( $\phi_{T,TPPS_4} = 0.75 \pm 0.02$ ,  $\phi_{T,ZnTMPyP} = 0.90 \pm 0.03$ ), and  $\phi_{T,ZnTPPS_4} = 0.89 \pm 0.03$ ) are highly compatible with the medium  $\phi_T$  values obtained using the known methods.

**Keywords:** triplet state quantum yield; photosensitizer; porphyrins; organic molecules; optical techniques; photophysical characterization



**Citation:** Borissevitch, I.E.; Silveira-Alves, E., Jr.; Almeida, C.G.L.; Souza, G.R.L.; Sokolov, S.S.; Gonçalves, P.J. An Alternative Method to Determine the Quantum Yield of the Excited Triplet State Using Laser Flash Photolysis.

*Photonics* **2023**, *10*, 409. <https://doi.org/10.3390/photonics10040409>

Received: 9 March 2023

Revised: 3 April 2023

Accepted: 4 April 2023

Published: 6 April 2023



**Copyright:** © 2023 by the authors. Licensee MDPI, Basel, Switzerland. This article is an open access article distributed under the terms and conditions of the Creative Commons Attribution (CC BY) license (<https://creativecommons.org/licenses/by/4.0/>).

## 1. Introduction

Triplet excited states ( $T_1$ ) play important roles in various photochemical processes, such as photocatalysis [1], photodynamic therapy (PDT) [2], the functioning of chromophoric dissolved organic matter (DCMO) [3], etc. The probability of triplet state formation per photon absorbed is described by the  $T_1$  quantum yield ( $\phi_T$ ) value, which is

one of the most important characteristics in the study of photochemical reactions. For these applications, it is of special interest to evaluate the photophysical characteristics of photoactive compounds (photosensitizers, PS) and to obtain the  $\varphi_T$  with high precision.

PDT is an effective medical technique for the treatment of various serious diseases, such as cancer and bacterial, fungal and viral infections [4–7]. This technique is based on the introduction of a PS to a patient's organism and its further excitation by visible light. The photodynamic action occurs via the photooxidation of living cell components, leading to cell death [2]. Photooxidation is realized either through the reaction of a biological target with radicals, formed by electron transfer between PS  $T_1$  (type I reactions) and a biological substrate, or through the reaction of the substrate with molecular oxygen in its excited singlet state (singlet oxygen, type II reactions), formed by energy transfer from the PS  $T_1$  state to molecular oxygen. Thus, the effectivity of the PS photodynamic action is dependent on the PS  $T_1$  state characteristics, its quantum yield being one of the most important characteristics. Therefore, information about the  $\varphi_T$  value is fundamental in the search for new and effective PSs.

Various experimental techniques, such as pulse radiolysis [8], photoacoustic technique [9,10], laser flash photolysis [11,12], time-resolved thermal lensing [13], picosecond laser double-pulse excitation [14], pulse train fluorescence and pulse train z-scan [15,16], are used to obtain the  $\varphi_T$  values. These techniques are based on different physical phenomena, such as ionizing radiation [8] and thermal, thermo-acoustic and optical effects [9–16]. Unfortunately, side effects, such as compound decomposition at high energy irradiation or thermal effects in the compound environment, can reduce the precision of the method.

Among these techniques, the Pulse Train Z-Scan (PTZS) technique is one of the most complete. PTZS is based on nonlinear optical effects, which are caused by the sample excitation with a sequence of intense picosecond pulses. In addition to the  $\varphi_T$  values, this technique allows the characteristics of the optical absorption and decay rate constants of the excited states to be obtained. PTZS is effective in studies of the photophysical properties of organic molecules, such as phthalocyanines [16,17], porphyrins [18], pH effects [19,20], solvent effects [21], aggregation effects [22,23], and the interaction with nanostructures, such as micelles [21,22], and macromolecules [24]. However, this technique requires very specific and complex laser systems containing multiple picosecond pulse sources, which are expensive and difficult to operate.

In contrast to PTZS, the Laser Flash Photolysis (LFP) technique is based on the excitation of a sample by an intense light pulse and the monitoring of its transient absorption using a continuous analyzing light beam. Being technically simpler than PTZS, LFP allows various sample characteristics to be determined, such as the  $\varphi_T$ , excited state absorption spectra and lifetimes and bimolecular rate constants, among others [11,12,25].

The discrepancy between the  $\varphi_T$  values obtained by different methods stimulates the analysis of various factors that can interfere with the process of determining the  $\varphi_T$  values. In the case of LFP, the inhomogeneity in the exciting laser pulse intensity can be one of the factors that can affect the  $\varphi_T$  value [26–28]. The spatial distribution (profile) of the laser pulse intensity leads to inhomogeneity in the concentration of excited molecules along the sample, which, in turn, should affect the intensity of the analyzing beam passing through the sample.

This makes it necessary to correct the transient absorption of the sample through the integral intensity of the excitation pulse. In the present work, we analyzed the effect of the intensity profile of the exciting laser pulse on the calculation of the  $\varphi_T$  value received using the LFP technique [29].

We analyzed the variation in the transient absorption of the sample as a function of the exciting laser pulse intensity and compared the results with those obtained by solving the rate equations of the five-level-energy diagram. To evaluate the proposed method, we used *meso*-tetra(4-sulfonatophenyl) porphine (TPPS<sub>4</sub>), its zinc complex (ZnTPPS<sub>4</sub>) and the zinc complex of *meso*-tetrakis(N-methylpyridinium-4-yl) (ZnTMPyP), which demonstrate high photodynamic activity and the photophysical parameters of which (excited states absorp-

tion cross-section, lifetimes and quantum yields) are well-known [20–22]. The  $\varphi_T$  values were determined through a comparison with the  $\varphi_T$  of *meso*-tetrakis(N-methylpyridinium-4-yl) (TMPyP), which was used as a standard.

## 2. Materials and Methods

Porphyrins were purchased from the Porphyrin Products Inc. Their solutions were prepared in phosphate buffer (PBS, pH 7.4). The UV-Vis absorption spectra were obtained using a double beam spectrophotometer Hitachi U-2900. The porphyrin concentrations were controlled spectrophotometrically using molar absorption coefficients:  $\epsilon_{01}^{\text{TPPS}_4}(\lambda = 515 \text{ nm}) = 1.30 \times 10^4 \text{ M}^{-1}$ ,  $\epsilon_{01}^{\text{TMPyP}}(\lambda = 518 \text{ nm}) = 1.39 \times 10^4 \text{ M}^{-1}$ ,  $\epsilon_{01}^{\text{ZnTPPS}_4}(\lambda = 556 \text{ nm}) = 1.74 \times 10^4 \text{ M}^{-1}$  and  $\epsilon_{01}^{\text{ZnTMPyP}}(\lambda = 563 \text{ nm}) = 1.74 \times 10^4 \text{ M}^{-1}$  [30].

The compound excited states were produced through the excitation of their solution in  $1.0 \times 1.0 \text{ cm}$  quartz cells with the second harmonic ( $\lambda_{\text{exc}} = 532 \text{ nm}$ ) from the Nd:YAG Brilliant Quantel System (Q-switched, 10 Hz repetition rate,  $\sim 7 \text{ ns}$  pulse width). The radius of the laser beam at the center of the cuvette is  $r_0 = 3.5 \text{ mm}$ .

The analyzing light beam was produced by a Lamp Bulb (XE075), 75 W Xenon Arc, Ozone Free light source with 75 W Xenon lamp, quartz collimator, light chopper and a computer-controlled monochromator from Sciencetech Inc (9055) coupled with a Photomultiplier tube Hamamatsu (R928). The direction of the analyzing light beam with radius  $l = 0.25 \text{ mm}$  was orthogonal to the pump beam. The transient absorption  $\Delta A$  was registered at  $\lambda_{\text{an}} = 470 \text{ nm}$ , where the optical absorption spectra of the porphyrin  $T_1$  state is more intense.

In all of the experiments, porphyrin solutions were freshly prepared before the measurements and the solution absorbance values were adjusted close to 0.2 at the excitation wavelength. To avoid the oxygen effects on the porphyrin triplet, the study was realized with de-aerated solutions after 30 min bubbling by nitrogen. The stability of the samples was confirmed using the absorption spectra before and after each LPF experiment, and just less than 5% degradation was observed. All experiments were carried out at room temperature  $\sim 26^\circ \text{C}$ .

The experimental data were treated using the OriginPro 8 commercial program. All final values were the average of three independent experiments.

## 3. Theoretical Model

Initially, in thermodynamic equilibrium, practically all PS molecules are in the ground state  $S_0$ . After the absorption of a photon, a PS molecule obtains excessive electronic energy, passing to the first singlet excited state  $S_1$ . The excess of  $S_1$  state energy may dissipate via three ways: fluorescence and internal conversion, through which the molecule returns to its initial  $S_0$  state; and intersystem crossing, which passes a molecule to the excited triplet state  $T_1$  [31]. Competition between these ways determines the  $T_1$  state quantum yield  $\varphi_T$ , defined as:

$$\varphi_T = \frac{n_{T_1}}{n_{\text{abs}}} \quad (1)$$

where  $n_{\text{abs}}$  is the number of photons absorbed by the sample and  $n_{T_1}$  is the number of molecules in the triplet state, formed by the absorption of these photons.

The  $\varphi_T$  value can be determined in two ways: (1) using the analysis of the kinetic characteristics of the  $S_1$  state energy dissipation; or (2) using the spectroscopic characteristics of the system after its excitation by light.

## 4. Determination of $\varphi_T$ Value from Kinetic Data

The kinetic analysis of the photophysical processes for typical PS molecules is based on solving the set of equations that describe the population fractions of electronic states as a function of time, which are written according to the five-energy level diagram, shown in Figure 1.

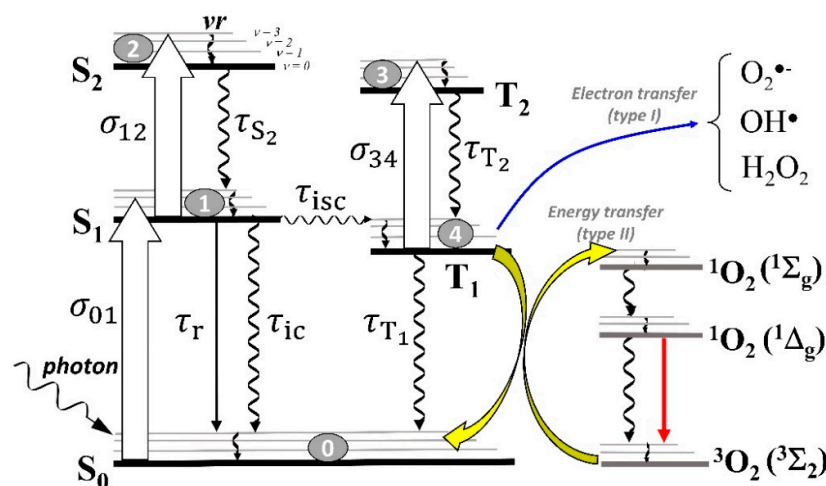


**Figure 1.** Five-level-energy diagram showing photophysical characteristics of a typical PS and the ROS production that occurs in the photodynamic application.  $S_i$  and  $T_i$  are the singlet and triplet states,  $\sigma_{ij}$  are the absorption cross-sections between  $i$  and  $j$  states.  $\tau$  are the lifetimes of the relaxation processes.

An equation rate set is given by:

$$\frac{dn_{S_0}}{dt} = -W_{01}n_{S_0} + \left( \frac{1}{\tau_r} + \frac{1}{\tau_{ic}} \right) n_{S_1} + \frac{n_{T_1}}{\tau_{T_1}} \quad (2a)$$

$$\frac{dn_{S_1}}{dt} = W_{01}n_{S_0} - \frac{n_{S_1}}{\tau_{S_1}} - W_{12}n_{S_1} + \frac{n_{S_2}}{\tau_{S_2}} \quad (2b)$$

$$\frac{dn_{S_2}}{dt} = W_{12}n_{S_1} - \frac{n_{S_2}}{\tau_{S_2}} \quad (2c)$$

$$\frac{dn_{T_1}}{dt} = \frac{n_{S_1}}{\tau_{isc}} - \frac{n_{T_1}}{\tau_{T_1}} - W_{34}n_{T_1} + \frac{n_{T_2}}{\tau_{T_2}} \quad (2d)$$

$$\frac{dn_{T_2}}{dt} = W_{34}n_{T_1} - \frac{n_{T_2}}{\tau_{T_2}} \quad (2e)$$

where  $W_{ij} = \sigma_{ij}I(t)/h\nu$  is the rate of the one-photon transition between  $i$  and  $j$  states,  $I(t)$  is the time-dependent irradiance of the laser pulse,  $h$  is the Planck's constant and  $\nu$  is the frequency of excitation.

The transition of a molecule from the  $S_0$  to  $S_1$  state is characterized by the absorption cross-sections  $\sigma_{01}(\lambda)$ , which depend on the wavelength of excitation ( $\lambda$ ). From the  $S_1$  state, electrons can be subsequently excited to a higher excited singlet state ( $S_1 \rightarrow S_2$  transition) during the laser pulse action, with an absorption cross-section  $\sigma_{12}(\lambda)$ . From the  $S_1$  state, a molecule can be deactivated through three processes: (i) decay to  $S_0$  via the radiative process (fluorescence, straight arrows); (ii) decay to  $S_0$  via the nonradiative process (wavy arrows) of internal conversion; or (iii) intersystem crossing to a triplet state  $T_1$ . These processes are characterized by lifetimes  $\tau_r$ ,  $\tau_{ic}$  and  $\tau_{isc}$ , respectively. A nonradiative transition, called vibrational relaxation ( $\nu r$ ), occurs from an upper vibrational level to the lowest one within the same electronic state.

In the triplet state  $T_1$ , the molecules can undergo one-photon absorption to the  $T_2$  state (absorption cross-section  $\sigma_{34}(\lambda)$ ) or relax to the  $S_0$  state. The lifetime of the  $T_1$  state ( $\tau_{T_1}$ ) is in the order of microseconds. The decay from the  $T_1$  state to  $S_0$  (represented by wavy arrows) occurs via radiative (phosphorescence) and nonradiative (reverse intersystem crossing) processes, the nonradiative process being dominant in solutions at room temperature.

In general, the decays of the  $S_2$  and  $T_2$  states are internal conversion processes, characterized by  $\tau_{S_2}$  and  $\tau_{T_2}$  lifetimes, which are very short (in the order of picoseconds). Therefore,  $S_1 \rightarrow S_2$  and  $T_1 \rightarrow T_2$  transitions do not affect the formation and decay of the  $T_1$  state.

The rate of the depopulation of the  $S_1$  state is:

$$\frac{dn_{S_1}}{dt} = -(k_r + k_{ic} + k_{isc})n_{S_1} \quad (3)$$

where  $k_i = \frac{1}{\tau_i}$  are the rate constants of the respective processes.

On the other hand, neglecting the depopulation of the  $T_1$  state, we can write its population as:

$$\frac{dn_{T_1}}{dt} = k_{isc}n_{S_1} \quad (4)$$

Combining Equations (3) and (4), we can obtain:

$$\frac{n_{T_1}}{n_{S_1}} = \frac{k_{isc}}{k_r + k_{ic} + k_{isc}} \quad (5)$$

At the same time,  $n_{S_1}$  is equal to the number of photons absorbed by system  $n_{abs}$ . Therefore, we can write:

$$\varphi_T = \frac{n_{T_1}}{n_{abs}} = \frac{k_{isc}}{k_r + k_{ic} + k_{isc}} \quad (6)$$

Thus, determining the set of rate constants of the  $S_1$  state depopulation, we can calculate the absolute value of the  $T_1$  state quantum yield  $\varphi_T$ .

However, the determination of this set of rate constants requires the use of complex experimental equipment, such as that used in nonlinear optics [20–22].

## 5. Determination of $\varphi_T$ Value from Spectroscopic Data

Figure 2 represents the scheme of propagation of the exciting and analyzing beams used for the calculation of the  $\varphi_T$  value from the spectroscopic data. For the calculation details, see “Supplementary Materials”.

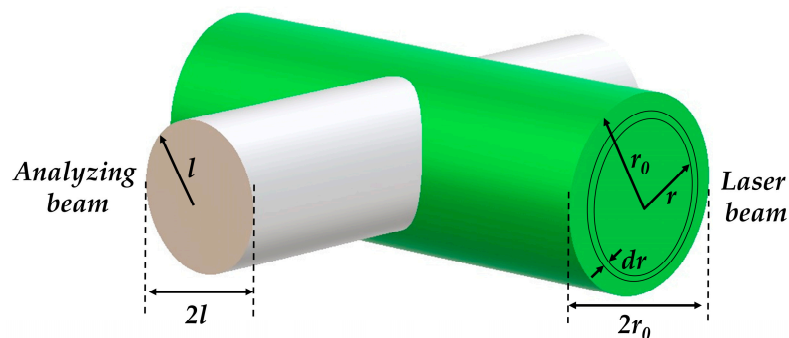


**Figure 2.** Scheme of propagation of the exciting and analyzing beams, used for calculation of  $\varphi_T$  value from spectroscopic data.

The exciting laser pulse beam, which has cylindrical symmetry with radius  $r_0$  and intensity distributed according to the Gaussian function, passes through the sample and excites the PS molecules. The continuous cylindrical analysis beam with radius  $l$  passes through the sample perpendicular to the direction of the exciting beam.

The number of exciting photons  $dn_{ex}(r, z)$  in the cylindrical volume element  $dV_r$  with radius  $r$  and height  $2l$

$$dV_r = 4\pi l r dr \quad (7)$$

is equal to

$$dn_{\text{ex}}(r, z) = GF(r, z)dV_r \quad (8)$$

where  $GF(r, z)$  is the Gaussian function.

Taking into account the fact that the laser pulse possesses cylindrical symmetry, the  $GF$  is presented in the form:

$$GF(r, z) = \frac{n_{\text{ex}0}}{4\pi l \zeta^2 \left[1 - \exp\left(-\frac{r_0^2}{2\zeta^2}\right)\right]} \exp\left(-\frac{r^2}{2\zeta^2}\right) \quad (9)$$

and

$$dn_{\text{ex}}(r, z) = \frac{n_{\text{ex}0}}{\zeta^2 \left[1 - \exp\left(-\frac{r_0^2}{2\zeta^2}\right)\right]} \exp\left(-\frac{r^2}{2\zeta^2}\right) r dr \quad (10)$$

where  $n_{\text{ex}0}$  is the number of photons in the center of the laser beam and  $\zeta$  is the half-width of the Gaussian function.

In accordance with the Lambert-Beer law, the number of absorbed photons is:

$$dn_{\text{abs}} = [1 - \exp(-\sigma_{01} N_0 2l)] dn_{\text{ex}}(r, z) = \frac{n_{\text{ex}0} [1 - \exp(-\sigma_{01} N_0 2l)]}{\zeta^2 \left[1 - \exp\left(-\frac{r_0^2}{2\zeta^2}\right)\right]} \exp\left(-\frac{r^2}{2\zeta^2}\right) r dr \quad (11)$$

where  $\sigma_{01}$  is the cross section of the  $S_0 \rightarrow S_1$  transition at the excitation wavelength and  $N_0$  is the number of PS molecules per volume unit.

Part of the molecule excited to the  $S_1$  state returns to the ground  $S_0$  state through fluorescence and internal conversion, while the other part passes to the  $T_1$  state via intersystem crossing. As the lifetime of the  $S_1$  state is in the order of nanoseconds, while the lifetime of the  $T_1$  state in liquid solutions is in the order of several hundred microseconds, soon after the end of the exciting pulse, only molecules in the  $S_0$  and  $T_1$  states are present in the sample. Molecules in the  $T_1$  state can also return to the  $S_0$  state through intersystem crossing and/or phosphorescence. However, as the lifetime of this process is much longer than the exciting pulse duration, the number of molecules in the  $T_1$  state can be considered constant during a certain time after the end of the exciting pulse [29].

It is necessary to note that the presence of molecular oxygen in liquid solutions drastically reduces the lifetime of the PS  $T_1$  state due to reactions between the PS molecule and oxygen [29] (Figure 1). Therefore, it is necessary to evacuate the oxygen from the solution to exclude this effect.

Finally, we can consider that over a long enough period compared with the exciting pulse duration, just two types of species are present in the sample: molecules in the  $S_0$  and  $T_1$  states.

In this case, the absorbance  $dA$  in the  $dr$  layer of the analyzing beam is:

$$dA = \sigma_S N_S dr + \sigma_T N_T dr \quad (12)$$

To distinguish the analyzing beam absorbance from that of the excitation laser pulse, the symbols  $\sigma_S$  and  $\sigma_T$  are used to represent the absorption cross-sections of the  $S_0 \rightarrow S_1$  and  $T_1 \rightarrow T_2$  transitions for the analyzing beam (at the analyzing wavelength).  $N_S = \frac{dn_S}{dV_r}$  and  $N_T = \frac{dn_T}{dV_r}$  are the numbers of PS molecules in the  $S_1$  and  $T_1$  states per volume unit, respectively.

Taking into account that  $N_S + N_T = N_0$  and combining with Equation (7), we can rewrite Equation (12) as:

$$d(\Delta A) = d(A - A_0) = (\sigma_T - \sigma_S) N_T dr = (\sigma_T - \sigma_S) \frac{dn_T}{4\pi l r dr} dr = (\sigma_T - \sigma_S) \frac{dn_T}{4\pi l r} \quad (12a)$$



where  $A_0 = \int_{-r_0}^{r_0} \sigma_S N_0 dr$  is the absorbance before the exciting pulse action.

Using the expressions (1) and (11), after integration, we obtain:

$$\Delta A = \varphi_T \frac{n_{ex0}(\sigma_T - \sigma_S)}{2\sqrt{2\pi}l\zeta} \frac{[1 - \exp(-\sigma_{01}N_0l)]}{\left[1 - \exp\left(-\frac{r_0^2}{2\zeta^2}\right)\right]} \operatorname{erf}\left(\frac{r_0}{\sqrt{2}\zeta}\right) \quad (12b)$$

where

$$\operatorname{erf}(x) = \frac{1}{\sqrt{\pi}} \int_0^{x^2} \exp(-t) \frac{dt}{\sqrt{t}}$$

is the error integral with the argument  $x = \frac{r_0}{\sqrt{2}\zeta}$ .

Finally,

$$\varphi_T = \frac{2\sqrt{2\pi}l\zeta}{n_{ex0}(\sigma_T - \sigma_S)} \frac{\left[1 - \exp\left(-\frac{r_0^2}{2\zeta^2}\right)\right]}{[1 - \exp(-\sigma_{01}N_0l)] \operatorname{erf}\left(\frac{r_0}{\sqrt{2}\zeta}\right)} \Delta A \quad (13)$$

Thus, to determine the absolute value of the  $\varphi_T$  from the spectroscopic data, it is necessary to take into account the distribution of the intensity in the exciting laser pulse.

However, the situation can be simplified using a standard compound at the same optical geometry. Indeed, the quantum yield of a standard is:

$$\varphi_T^s = \frac{2\sqrt{2\pi}l\zeta}{n_{ex0}^s(\sigma_T^s - \sigma_S^s)} \frac{\left[1 - \exp\left(-\frac{r_0^2}{2\zeta^2}\right)\right]}{[1 - \exp(-\sigma_{01}^s N_0^s l)] \operatorname{erf}\left(\frac{r_0}{\sqrt{2}\zeta}\right)} \Delta A^s \quad (13a)$$

and

$$\varphi_T = \frac{n_{ex0}^s (\sigma_T^s - \sigma_S^s)}{n_{ex0} (\sigma_T - \sigma_S)} \frac{[1 - \exp(-\sigma_{01}^s N_0^s l)]}{[1 - \exp(-\sigma_{01} N_0 l)]} \frac{\Delta A}{\Delta A^s} \varphi_T^s \quad (14)$$

The exciting pulse energy being the same for the sample and the standard ( $n_{ex0} = n_{ex0}^s$ ), then:

$$\varphi_T = \frac{(\sigma_T^s - \sigma_S^s)}{(\sigma_T - \sigma_S)} \frac{[1 - \exp(-\sigma_{01}^s N_0^s l)]}{[1 - \exp(-\sigma_{01} N_0 l)]} \frac{\Delta A}{\Delta A^s} \varphi_T^s \quad (14a)$$

In this case, the calculation of the  $\varphi_T$  is independent of the characteristics of the exciting pulse.

The situation is even simpler if the sample and the standard absorbances in the exciting beam direction,  $\sigma_{01} N_0 l$  and  $\sigma_{01}^s N_0^s l$ , are both  $\ll 1$ . In this case, the  $\varphi_T$  can be expressed as:

$$\varphi_T = \frac{(\sigma_T^s - \sigma_S^s)}{(\sigma_T - \sigma_S)} \frac{\sigma_{01}^s N_0^s}{\sigma_{01} N_0} \frac{\Delta A}{\Delta A^s} \varphi_T^s \quad (14b)$$

A serious problem lies in the definition of the  $(\sigma_T - \sigma_S)$  and  $(\sigma_T^s - \sigma_S^s)$  values. In general, they can be calculated by Equation (12a) when the energy of the exciting pulse is high; therefore, all of the excited molecules pass to the triplet state. In this case,  $N_T = N_0$  (saturation) and

$$(\sigma_T - \sigma_S) = \frac{\Delta A_{\max}}{N_0} \quad (15)$$

where  $\Delta A_{\max}$  is the  $\Delta A$  limit value for the pulse energy  $\rightarrow \infty$ .

However, it is unlikely that saturation can be achieved on the border of the exciting beam where its intensity is very low as compared with that in the beam center. This can explain the significant dispersion in the  $\varphi_T$  values obtained in different studies.

On the other hand, the kinetic analysis demonstrates that the  $N_T$  dependence on the exciting pulse energy is exponential. Therefore, we can use the exponential approximation to determine the  $\Delta A_{\max}$  as the limit of this exponential function for the pulse energy  $\rightarrow \infty$ .

Combining Equations (14b) and (15), we obtain:

$$\varphi_T = \frac{\Delta A_{\max}^s \sigma_{01}^s}{\Delta A_{\max} \sigma_{01}} \frac{\Delta A}{\Delta A^s} \varphi_T^s \quad (16)$$

Replacing the cross-sections  $\sigma_{01}$  by the molar absorption coefficients  $\varepsilon_{01}$  ( $\sigma_{01} = \frac{2303}{N_A} \varepsilon_{01}$ , where  $N_A$  is the Avogadro constant), we can transform Equation (16) to a form more adequate for spectroscopy. Taking into account that  $\varepsilon = \frac{A}{CL}$ , where  $A$  is the absorbance,  $C$  is the sample concentration in M and  $L$  is the optical pass within the sample in cm, we can rewrite Equation (16) as:

$$\varphi_T = \frac{\Delta A_{\max}^s A_{\text{ex}}^s C^s}{\Delta A_{\max} A_{\text{ex}} C} \frac{\Delta A}{\Delta A^s} \varphi_T^s \quad (16a)$$

where  $A_{\text{ex}}$  and  $A_{\text{ex}}^s$  are the absorbances of the sample and the standard at the excitation wavelength, and  $C$  and  $C^s$  are the PS concentrations in the sample and in the standard, respectively.

All of the parameters in Equation (16a), except  $\Delta A^s$  and  $\Delta A$ , are determined independently and are independent of the exciting pulse energy. Thus, varying the exciting pulse energy, we can obtain the  $\Delta A$  values in the function of  $\Delta A^s$ , and determine the  $\varphi_T$  from the  $\Delta A$  dependence on  $\Delta A^s$ :

$$\varphi_T = B \frac{\Delta A}{\Delta A^s} \varphi_T^s \quad (17)$$

where  $B = \frac{\Delta A_{\max}^s A_{\text{ex}}^s C^s}{\Delta A_{\max} A_{\text{ex}} C}$

The procedure of the  $\varphi_T$  determination consists of four steps:

- (i) The amplitudes of the  $T_1$  state decay kinetic curves ( $\Delta A$  and  $\Delta A^s$ ) are measured in the function of the exciting pulse energy ( $E$ ) for the sample and the standard.
- (ii) The dependences of  $\Delta A$  and  $\Delta A^s$  on the energy are fitted in accordance with an exponential function. From this fitting, the values of  $\Delta A_{\max}$  and  $\Delta A_{\max}^s$  are obtained.
- (iii) The obtained fittings are used to determine  $\Delta A$  and  $\Delta A^s$  for the same exciting energy.
- (iv) The dependence of  $\Delta A$  upon  $\Delta A^s$  is constructed.

## 6. Results and Discussions

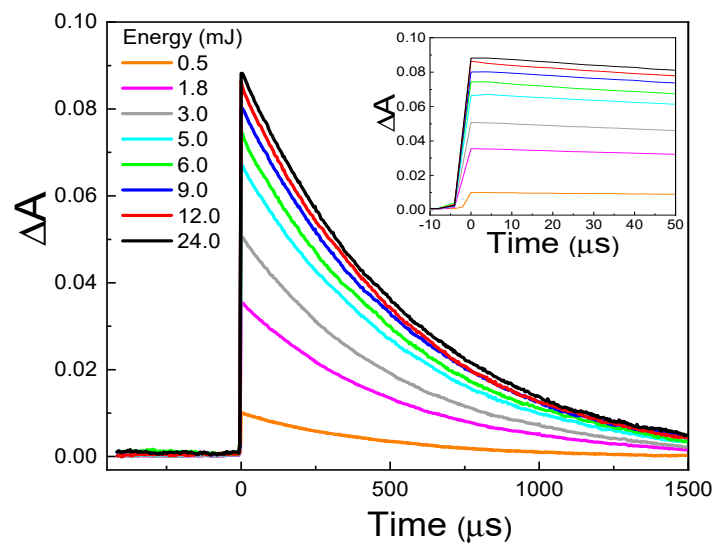
The  $T_1$  state quantum yields ( $\varphi_T$ ) were determined through a comparison with a standard. TMPyP porphyrin was chosen as a standard as its  $\varphi_T$  was measured using various methods. We used TMPyP  $\varphi_T = 0.82 \pm 0.08$ , calculated as an average of the  $\varphi_T$ , obtained in various studies found in the literature [8,15,21,32,33].

Figure 3 demonstrates the kinetic curves of the TMPyP porphyrin  $T_1$  decay for different laser pulse energies.

Figure 4 shows the  $\Delta A$  for the studied porphyrins in the function of the laser pulse energy and the respective exponential approximation curves. The insets on Figure 4b–d demonstrate the  $\Delta A$  in the function of  $\Delta A^s$  for each studied porphyrin. The  $\Delta A \times \Delta A^s$  curves (inset of Figure 4b–d) were fitted in the range of low exciting energy, where this dependence is linear. The use of five points for fitting was enough to obtain a statistically significant result.

The triplet quantum yield values, obtained using the proposed method, are listed in Table 1 ( $\varphi_T^*$ ). A good accordance can be observed with the average values obtained using the Pulse Radiolysis technique [8] and through various modifications of the Laser Flash-Photolysis technique [32,34–38] (last column of Table 1,  $\varphi_T^{***}$ ).





**Figure 3.** Decay kinetic curves of the TMPyP triplet state  $T_1$  for different exciting pulse energies (probe wavelength at 470 nm).

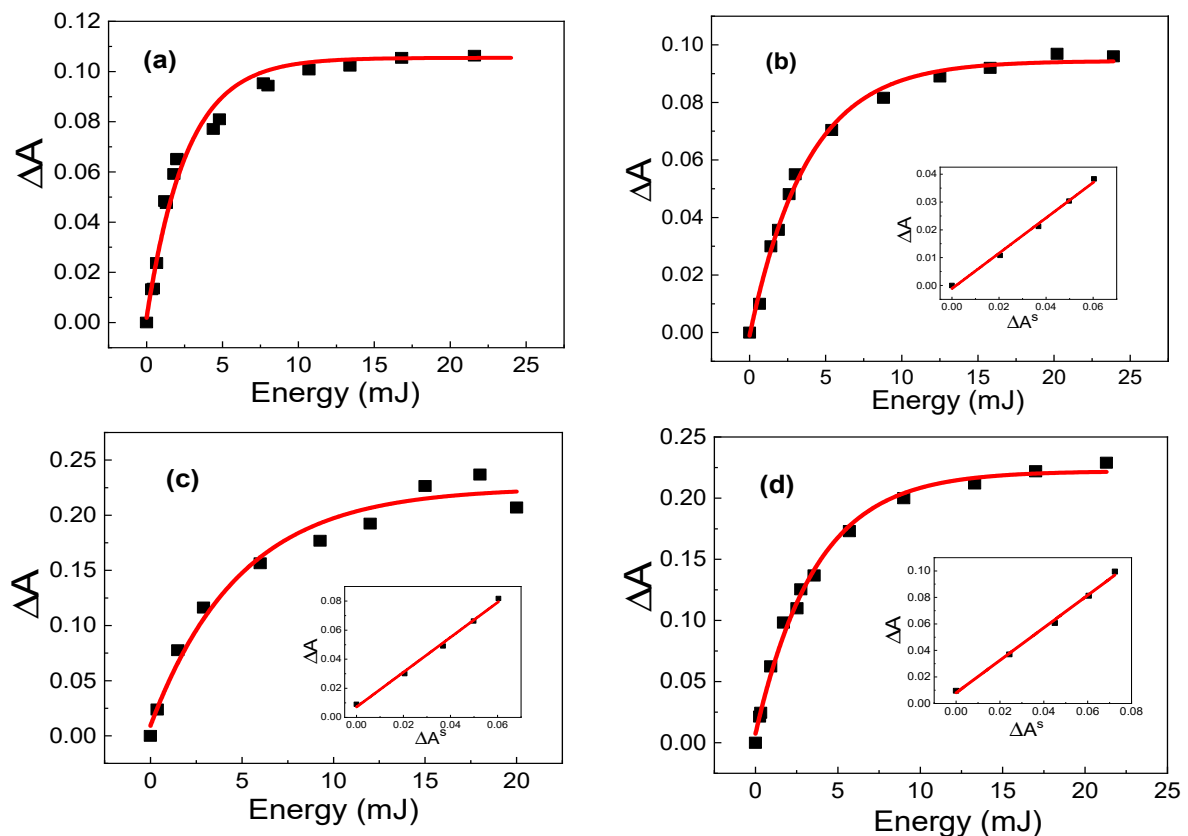


**Figure 4.** Transient absorption  $\Delta A$  in function of the exciting pulse energy for: (a) TMPyP, (b) TPPS<sub>4</sub>, (c) ZnTMPyP and (d) ZnTPPS<sub>4</sub>. Insets:  $\Delta A$  as a function of  $\Delta A^s$ .

For ZnTMPyP, there is a certain discrepancy between the values obtained using the proposed method ( $\phi_T^*$ ) and the kinetic analysis ( $\phi_T^{**}$ ) obtained using the Pulse Train Z-Scan (PTZS) technique. This difference can be explained by the fact that the PTZS technique requires a high molar concentration of porphyrin, where ZnTMPyP aggregation can occur, reducing the effective  $\phi_T$  value. The LFP technique uses low porphyrin concentrations, which reduces the probability of aggregation, and provides the determination of the real

$\varphi_T$  value for the monomer. Moreover, an increase in the scattered light intensity for high compound concentrations can also cause certain discrepancies in the  $\varphi_T$  values.

**Table 1.** Parameters used to calculate the triplet quantum yield in accordance with equation (16a), quantum yield values, determined in this study ( $\varphi_T^*$ ), obtained from the kinetic analysis ( $\varphi_T^{**}$ ) and average values, calculated from literature ( $\varphi_T^{***}$ ).

Sample	C <sub>s</sub> ( $\mu$ M)	C ( $\mu$ M)	A <sub>ex</sub> <sup>s</sup>	A <sub>ex</sub>	$\Delta A_{\max}$	$\Delta A_{\max}^s$	$\frac{\Delta A}{\Delta A^s}$	$\varphi_T^*$	$\varphi_T^{**}$	$\varphi_T^{***}$
TPPS <sub>4</sub>	25.0	37.2	0.194	0.195	0.094	0.101	0.574	0.75 ( $\pm 0.02$ )	0.77 <sup>a</sup> ( $\pm 0.05$ )	0.77 <sup>c</sup> ( $\pm 0.02$ )
ZnTMPyP	28.9	64.0	0.234	0.245	0.225	0.108	1.087	0.90 ( $\pm 0.03$ )	0.7 <sup>b</sup> ( $\pm 0.2$ )	0.90 <sup>d</sup> ( $\pm 0.00$ )
ZnTPPS <sub>4</sub>	25.0	49.1	0.194	0.182	0.221	0.101	1.132	0.89 ( $\pm 0.03$ )	0.8 <sup>b</sup> ( $\pm 0.2$ )	0.86 <sup>e</sup> ( $\pm 0.01$ )

$\varphi_T^*$ —triplet quantum yields, obtained in this work using TMPyP as a standard with the  $\varphi_T^S$  average value  $0.82 \pm 0.08$  ( $\pm$ SD), refs.: [8,15,21,32,33].  $\varphi_T^{**}$ —triplet quantum yields, determined from the kinetic analysis: <sup>a</sup> ref [20], <sup>b</sup> ref [22].  $\varphi_T^{***}$ —average values calculated from: <sup>c</sup> refs: [8,32]; <sup>d</sup> refs: [32,34,35]; <sup>e</sup> refs.: [32,36–38].

## 7. Conclusions

In the present work, we demonstrate the importance of the intensity profile of the exciting laser pulse for the process of determining the triplet state quantum yield ( $\varphi_T$ ) using the Laser Flash Photolysis technique. We propose an alternative method to obtain the  $\varphi_T$  value, using a standard based on the analysis of the variation of the transient absorption of the sample in the function of the intensity of the exciting laser pulse. The final equation, with the exception of the transient absorptions of the sample ( $\Delta A$ ) and the standard ( $\Delta A^s$ ), includes only those parameters that do not depend on the exciting pulse energy, which can be determined independently. An important aspect of the proposed method is that the  $\frac{\Delta A}{\Delta A^s}$  ratio is calculated from exponential approximations of the  $\Delta A$  and  $\Delta A^s$  dependences on the exciting pulse energy. This excludes the difference between the exciting energies for the  $\Delta A$  and  $\Delta A^s$  and the necessity to determine the  $\Delta A$  and  $\Delta A^s$  at a high pulse energy (saturation), thus reducing the deviation in the process of the  $\varphi_T$  calculation. The viability of the proposed method is confirmed by the fact that the obtained  $\varphi_T$  values coincide with the average  $\varphi_T$  values calculated from the data published in the literature.

**Supplementary Materials:** The following supporting information can be downloaded at: <https://www.mdpi.com/article/10.3390/photonics10040409/s1>, SI-1: Scheme of propagation of the exciting and analyzing beams, used for calculation of  $\varphi_T$  value from spectroscopic data.

**Author Contributions:** Conceptualization, I.E.B. and P.J.G.; methodology, I.E.B., E.S.-A.J., C.G.L.A. and P.J.G.; software, C.G.L.A.; validation, I.E.B., E.S.-A.J., S.S.S. and P.J.G.; formal analysis, I.E.B., E.S.-A.J., G.R.L.S., S.S.S. and P.J.G.; investigation, I.E.B., E.S.-A.J., S.S.S. and P.J.G.; resources, I.E.B., G.R.L.S. and P.J.G.; data curation, I.E.B., S.S.S. and P.J.G.; writing—original draft preparation, I.E.B. and P.J.G.; writing—review and editing, I.E.B., G.R.L.S. and P.J.G.; visualization, I.E.B., G.R.L.S. and P.J.G.; supervision, I.E.B. and P.J.G.; project administration, I.E.B. and P.J.G.; funding acquisition, I.E.B., G.R.L.S. and P.J.G. All authors have read and agreed to the published version of the manuscript.

**Funding:** This research was funded, and the authors gratefully acknowledge financial support from Fundação de Amparo à Pesquisa do Estado de Goiás (FAPEG grants: 201410267001776 and 201710267000533); Conselho Nacional de Desenvolvimento Científico e Tecnológico (CNPq); and Coordenação de Aperfeiçoamento de Pessoal de Nível Superior (CAPES: 88882.386417/2019-01).

**Institutional Review Board Statement:** Not applicable.

**Informed Consent Statement:** Not applicable.

**Data Availability Statement:** The data presented in this study are available on request from the corresponding author.

**Acknowledgments:** The authors are grateful to Galina Borissevitch for valuable discussions and the English proofreading of our manuscript.

**Conflicts of Interest:** The authors declare no conflict of interest.

## References

- Strieth-Kalthoff, F.; Glorius, F. Triplet Energy Transfer Photocatalysis: Unlocking the Next Level. *Chem* **2020**, *6*, 1888–1903. [CrossRef]
- Kwiatkowski, S.; Knap, B.; Przystupski, D.; Saczko, J.; Kędzierska, E.; Knap-Czop, K.; Kotlińska, J.; Michel, O.; Kotowski, K.; Kulbacka, J. Photodynamic therapy—Mechanisms, photosensitizers and combinations. *Biomed. Pharmacother.* **2018**, *106*, 1098–1107. [CrossRef] [PubMed]
- Miao, S.; Lyu, H.; Xu, J.; Bi, S.; Guo, H.; Mu, M.; Lei, S.; Zeng, S.; Liu, H. Characteristics of the chromophoric dissolved organic matter of urban black-odor rivers using fluorescence and UV-visible spectroscopy. *Environ. Pollut.* **2021**, *268*, 115763. [CrossRef]
- National Cancer Institute. Photodynamic Therapy to Treat Cancer. Available online: <https://www.cancer.gov/about-cancer/treatment/types/photodynamic-therapy> (accessed on 10 January 2023).
- Liu, Y.; Qin, R.; Zaat, S.A.J.; Breukink, E.; Heger, M. Antibacterial photodynamic therapy: Overview of a promising approach to fight antibiotic-resistant bacterial infections. *J. Clin. Transl. Res.* **2015**, *1*, 140–167. [PubMed]
- Conrado, P.C.V.; Sakita, K.M.; Arita, G.S.; Galinari, C.B.; Gonçalves, R.S.; Lopes, L.D.G.; Lonardoni, M.V.C.; Teixeira, J.J.V.; Bonfim-Mendonça, P.S.; Kioshima, E.S. A systematic review of photodynamic therapy as an antiviral treatment: Potential guidance for dealing with SARS-CoV-2. *Photodiagn. Photodyn. Ther.* **2021**, *34*, 102221. [CrossRef] [PubMed]
- Lyon, J.P.; Moreira, L.M.; de Moraes, P.C.; dos Santos, F.V.; de Resende, M.A. Photodynamic therapy for pathogenic fungi. *Mycoses* **2011**, *54*, e265–e271. [CrossRef]
- Bonnet, R.; Ridge, R.J.; Land, E.J.; Sinclair, R.S.; Tait, D.; Truscott, T.G. Pulsed irradiation of water-soluble porphyrins. *J. Chem. Soc. Faraday Trans. Phys. Chem. Condens. Phases* **1982**, *78*, 127–136. [CrossRef]
- Pineiro, M.; Carvalho, A.L.; Pereira, M.M.; Gonsalves, A.M.R.; Arnaut, L.G.; Formosinho, S.J. Photoacoustic measurements of porphyrin triplet-state quantum yields and singlet-oxygen efficiencies. *Chemistry* **1998**, *4*, 2299–2307. [CrossRef]
- Fletcher, B.; Grabowski, J.J. Photoacoustic calorimetry—An undergraduate physical-organic experiment. *J. Chem. Educ.* **2000**, *77*, 640–645. [CrossRef]
- Bensasson, R.; Goldschmidt, R.; Land, E.J.; Truscott, T.G. Laser Intensity and the Comparative Method for Determination of Triplet Quantum Yield. *Photochem. Photobiol.* **1978**, *28*, 277–281. [CrossRef]
- Carmichael, I.; Hug, G.L. Triplet–Triplet Absorption Spectra of Organic Molecules in Condensed Phases. *J. Phys. Chem. Ref. Data* **1986**, *15*, 321–426. [CrossRef]
- Harada, Y.; Suzuki, T.; Ichimura, T.; Xu, Y.Z. Triplet formation of 4-thiothymidine and its photosensitization to oxygen studied by time-resolved thermal lensing technique. *J. Phys. Chem. B* **2007**, *111*, 5518–5524. [CrossRef] [PubMed]
- Reindl, S.; Penzkofer, A. Triplet quantum yield determination by picosecond laser double-pulse fluorescence excitation. *Chem. Phys.* **1996**, *213*, 429–438. [CrossRef]
- De Boni, L.; Franzen, P.L.; Gonçalves, P.J.; Borissevitch, I.E.; Misoguti, L.; Mendonça, C.R.; Zilio, S.C. Pulse train fluorescence technique for measuring triplet state dynamics. *Opt. Express* **2011**, *19*, 10814. [CrossRef] [PubMed]
- Mendonça, C.R.; Gaffo, L.; Misoguti, L.; Moreira, W.C.; Oliveira, O.N., Jr.; Zilio, S.C. Characterization of dynamic optical nonlinearities in ytterbium bis-phthalocyanine solution. *Chem. Phys. Lett.* **2000**, *323*, 300–304. [CrossRef]
- Cocca, L.H.Z.; Oliveira, T.M.A.; Gotardo, F.; Teles, A.V.; Menegatti, R.; Siqueira, J.P.; Mendonça, C.R.; Bataus, L.A.M.; Ribeiro, A.O.; Souza, T.F.M.; et al. Tetracarboxy-phthalocyanines: From excited state dynamics to photodynamic inactivation against Bovine herpesvirus type 1. *J. Photochem. Photobiol. B* **2017**, *175*, 1–8. [CrossRef]
- Cocca, L.H.Z.; Gotardo, F.; Sciuti, L.F.; Acunha, T.V.; Iglesias, B.A.; De Boni, L. Investigation of excited singlet state absorption and intersystem crossing mechanism of isomeric meso-tetra(pyridyl)porphyrins containing peripheral polypyridyl platinum(II) complexes. *Chem. Phys. Lett.* **2018**, *708*, 1–10. [CrossRef]
- De Boni, L.; Monteiro, C.J.P.; Mendonça, C.R.; Zílio, S.C.; Gonçalves, P.J. Influence of halogen atoms and protonation on the photophysical properties of sulfonated porphyrins. *Chem. Phys. Lett.* **2015**, *633*, 146–151. [CrossRef]
- Gonçalves, P.J.; De Boni, L.; Barbosa Neto, N.M.; Rodrigues, J.J., Jr.; Zilio, S.C.; Borissevitch, I.E. Effect of protonation on the photophysical properties of meso-tetra(sulfonatophenyl) porphyrin. *Chem. Phys. Lett.* **2005**, *407*, 236–241. [CrossRef]
- Gonçalves, P.J.; Franzen, P.L.; Correa, D.S.; Almeida, L.M.; Takara, M.; Ito, A.S.; Zilio, S.C.; Borissevitch, I.E. Effects of environment on the photophysical characteristics of mesotetrakis methylpyridiniumyl porphyrin (TMPyP). *Spectrochim. Acta Part A* **2011**, *79*, 1532–1539. [CrossRef]
- Gonçalves, P.J.; Corrêa, D.S.; Franzen, P.L.; De Boni, L.; Almeida, L.M.; Mendonça, C.R.; Borissevitch, I.E.; Zilio, S.C. Effect of interaction with micelles on the excited-state optical properties of zinc porphyrins and J-aggregates formation. *Spectrochim. Acta Part A* **2013**, *112*, 309–317. [CrossRef] [PubMed]
- Gonçalves, P.J.; Barbosa Neto, N.M.; Parra, G.G.; de Boni, L.; Aggarwal, L.P.F.; Siqueira, J.P.; Misoguti, L.; Borissevitch, I.E.; Zilio, S.C. Excited-state dynamics of meso-tetrakis(sulfonatophenyl) porphyrin J-aggregates. *Opt. Mater.* **2012**, *34*, 741–747. [CrossRef]

24. Gonçalves, P.J.; Bezerra, F.C.; Almeida, L.M.; Alonso, L.; Souza, G.R.L.; Alonso, A.; Zílio, S.C.; Borissevitch, I.E. Effects of bovine serum albumin (BSA) on the excited-state properties of meso-tetrakis(sulfonatophenyl) porphyrin (TPPS<sub>4</sub>). *Eur. Biophys. J.* **2019**, *48*, 721–729. [[CrossRef](#)] [[PubMed](#)]
25. Borissevitch, I.E.; Ferreira, L.P.; Gonçalves, P.J.; Amado, A.M.; Schlothauer, J.C.; Baptista, M.S. Quenching of meso-tetramethylpyridyl porphyrin excited triplet state by inorganic salts: Exciplex formation. *J. Photochem. Photobiol. A* **2018**, *367*, 156–161. [[CrossRef](#)]
26. Dóka, E.; Lente, G. Modeling Studies of Inhomogeneity Effects during Laser Flash Photolysis Experiments: A Reaction–Diffusion Approach. *J. Phys. Chem. A* **2017**, *121*, 2740–2747. [[CrossRef](#)]
27. Bazin, M.; Ebbesen, T.W. Distortions in Laser Flash Photolysis Absorption Measurements. The Overlap Problem. *Photochem. Photobiol.* **1983**, *37*, 675–678. [[CrossRef](#)]
28. Goetz, M.; Fehse, D.; Brauttsch, M. Laser flash photolysis with back-reflected excitation light—Analysis and experimental verification of the improvements in excitation intensity and homogeneity by a retroreflector. *J. Photochem. Photobiol. A* **2013**, *262*, 1–6. [[CrossRef](#)]
29. Zhang, X.F. Laser flash photolysis. In *Encyclopedia of Physical Organic Chemistry*, 1st ed.; Wang, Z., Ed.; John Wiley & Sons, Inc.: Hoboken, NJ, USA, 2017; ISBN 978-1-118-46858-6.
30. Teles, A.V.; Oliveira, T.M.A.; Bezerra, F.C.; Alonso, L.; Alonso, A.; Borissevitch, I.E.; Gonçalves, P.J.; Souza, G.R.L. Photodynamic inactivation of Bovine herpesvirus type 1 (BoHV-1) by porphyrins. *J. Gen. Virol.* **2018**, *99*, 1301–1306. [[CrossRef](#)]
31. Turro, N.J. *Modern Molecular Photochemistry*; Benjamin-Cummings: Menlo Park, CA, USA, 1978; 628p.
32. Kalyanasundaram, K.; Neumann-Spallart, M. Photophysical and redox properties of water-soluble porphyrins in aqueous media. *J. Phys. Chem.* **1982**, *86*, 5163–5169. [[CrossRef](#)]
33. Chirvony, V.S.; Galievsky, V.A.; Kruk, N.N.; Dzhagarov, B.M.; Turpin, P.Y. Photophysics of cationic 5,10,15,20-tetrakis-(4-N-methylpyridyl) porphyrin bound to DNA, [poly(dA-dT)]<sub>2</sub> and [poly(dG-dC)]<sub>2</sub>: On a possible charge transfer process between guanine and porphyrin in its excited singlet state. *J. Photochem. Photobiol. B* **1997**, *40*, 154–162. [[CrossRef](#)]
34. Harriman, A.; Porter, G.; Richou, M.C. Photosensitised Reduction of Water to Hydrogen using Water-soluble Zinc Porphyrins. *J. Chem. Soc. Faraday Trans.* **1981**, *77*, 833–844. [[CrossRef](#)]
35. Kalyanasundaram, K. Photochemistry of Water-Soluble Porphyrins: Comparative Study of Isomeric Tetrapyrrolyl- and Tetrakis(N-Methylpyridiniumyl) porphyrins. *Inorg. Chem.* **1984**, *23*, 2453–2459. [[CrossRef](#)]
36. Kubat, P.; Mosinger, J. Photophysical properties of metal complexes of meso-tetrakis (4-sulphonatophenyl) porphyrin. *J. Photochem. Photobiol. A* **1996**, *96*, 93–97. [[CrossRef](#)]
37. Mosinger, J.; Kliment, V.; Sejbál, J.; Kubát, P.; Lang, K. Host-guest complexes of anionic porphyrin sensitizers with cyclodextrins. *J. Porphyr. Phthalocyanines* **2002**, *6*, 514. [[CrossRef](#)]
38. Mosinger, J.; Micka, Z. Quantum yields of singlet oxygen of metal complexes of meso-tetrakis(sulphonatophenyl) porphine. *J. Photochem. Photobiol. A* **1997**, *107*, 77–82. [[CrossRef](#)]

**Disclaimer/Publisher's Note:** The statements, opinions and data contained in all publications are solely those of the individual author(s) and contributor(s) and not of MDPI and/or the editor(s). MDPI and/or the editor(s) disclaim responsibility for any injury to people or property resulting from any ideas, methods, instructions or products referred to in the content.